CARBON 61 (2013) 602–608

Available at www.sciencedirect.com

SciVerse ScienceDirect

journal homepage: www.elsevier.com/locate/carbon

# Variation of temperature dependence of electrical resistivity with crystal structure of artificial graphite products

Norio Iwashita [a,*], Hiroshi Imagawa [b], Wataru Nishiumi [b]

[a] National Institute of Advanced Industrial Science and Technology, AIST, Tsukuba 305-8568, Japan
[b] SEC Carbon Ltd., Fukuchiyama, 620-0853 Kyoto, Japan

ARTICLE INFO

*Article history:*
Received 26 March 2013
Accepted 20 May 2013
Available online 31 May 2013

ABSTRACT

Electrical resistivity of 12 artificial graphite products was measured by 4-pin probe constant current method in argon atmosphere in a furnace, in the temperature range from ambient to 1200 °C. In order to study the effects of crystal structure of the graphite products on their electric properties, X-ray diffraction (XRD) structural parameters, such as, average interlayer spacing ($d_{002}$), crystallite sizes (*Lc* and *La*) and graphitization degree ($P_1$), were measured by the methodology as outlined in JIS R7651. For the temperature dependence of resistivity of these products, it was observed that the minimum resistivity was located at the temperature ranges from 450 to 700 °C. From the relationship between the temperature dependence of resistivity and XRD structural parameters of the graphite products, some control factors of electrical properties at high temperature was discussed. Between the electrical resistivity at ambient temperature and $P_1$, a mutual relationship could be observed. It was seen that the normalized value of the minimum from the ambient resistivity was related with $d_{002}$. The temperature showing the minimum resistivity was lowered with enlargement of crystallite size along the *a*-axis, *La*. The slope of temperature dependence of resistivity at 1000 °C showed a correlation with *La*.



## 1. Introduction

Many artificial graphite materials are utilized at a high temperature for refining such as steel, aluminum and silicon semiconductor, etc. For such applications, it is important to understand the physical properties of carbon materials under high temperatures. The electrical resistivity of artificial graphite products is strongly dependent on their crystal structure and texture. Applying the graphite products to these manufacturing industries, dependences of its electrical resistance on the temperature are keys for the optimization of the manufacturing condition. Thermal conductivity and electrical resistivity of graphite materials from ambient temperature to high temperature have been reported in the 1970s [1–3]. For example, Lutcov et al. [1], reported the results of measurements of thermal conductivity, electrical resistivity and heat capacity of graphite materials with different bulk density under the high temperature range 50–2500 K. It was shown that the temperature dependences of these properties changed with the bulk density. Bapat et al. [2,3] reported unique variations of thermal conductivity and electrical resistivity of commercial artificial graphite materials (POCO graphite) to 3300 K. Beside these reports, however, there were almost no systematic studies on electrical resistance at the higher temperature of artificial graphite products. Moreover, there were no detailed descriptions of any information on the instrumentation of measurement of resistance in high temperature in these papers.

* *Corresponding author:* Fax: +81 29 861 5881.
E-mail address: n-iwashita@aist.go.jp (N. Iwashita).
0008-6223/$ - see front matter 
http://dx.doi.org/10.1016/j.carbon.2013.05.042

One of authors (Iwashita) has developed some special instruments for the measurement of physical properties of carbon materials at high temperature above 2000 °C in Argon atmosphere and reported mechanical tests [4–7], electrical resistance [4] and thermal diffusivity [8] at the high temperature range from ambient to 2600 °C. For a dozen artificial graphite products manufactured by SEC Carbon Ltd., in the present work, the temperature dependences of electric resistivity were measured from ambient temperature to 1200 °C. The controlling factors of the temperature dependences of resistivity were discussed from some XRD structural parameters of the graphite products.

## 2. Experimental

Twelve types of manufactured graphite products were used in this work. The graphite products manufactured from several types of fillers and binder pitches via press extruding process. Petroleum cokes were used as the fillers, and binder was coal tar pitch. Bulk density of these products is listed in Table 1. The XRD structural parameters, average interlayer spacing ($d_{002}$) and crystallite sizes (Lc and La) of these graphite products were measured by the methodology as outlined in JIS R7651 [9]. For each parameter, five times XRD measurements were carried out to calculate their mean values. The graphitization degree ($P_1$) of these products is analyzed from 11 diffraction profile by following the method with Warren and Houska [10,11]. The perfect graphitic structure means $P_1 = 1$, and the perfect turbostratic structure $P_1 = 0$. For many kinds of carbon material, the relation between graphitization degree $P_1$ and other XRD structural parameters was already reported [12–14].

Electrical resistance measurement was carried out by 4-pin probe constant current method in the electrical furnace [4]. The specimen size was $10 \times 10 \times 120$ mm. In the specimen, its longitudinal direction was the same as the extruding press of the graphite products. The specimen was held on isotropic graphite jigs as the current probe, as shown in Fig. 1. The distance between two probe pins for the measurement of voltage is 52 mm, fixing by the graphite screws. The special electric furnace with graphite heater was controlled to heat up to 1200 °C, measured by both thermocouple and pyrometer. The electrical resistance was continuously measured during cooling down to an ambient temperature. When the constant current of ±100 mA was applied to the specimen, the voltage difference was measured by a computer system with sampling every 1 min. The calibration of the measurement system was carried out using the standard resistor of 10 mΩ before the measurement every time. Two measurements of high temperature resistance were carried out for each graphite product. For calculating the resistivity, the length change by thermal expansion was not taken into account, using the length measured at ambient temperature.

**Table 1 – Bulk density of graphite products.**

| Sample | Bulk density (M kg/m$^3$) |
|---|---|
| 1 | 1.73 |
| 2 | 1.68 |
| 3 | 1.71 |
| 4 | 1.71 |
| 5 | 1.67 |
| 6 | 1.64 |
| 7 | 1.67 |
| 8 | 1.71 |
| 9 | 1.71 |
| 10 | 1.75 |
| 11 | 1.65 |
| 12 | 1.65 |

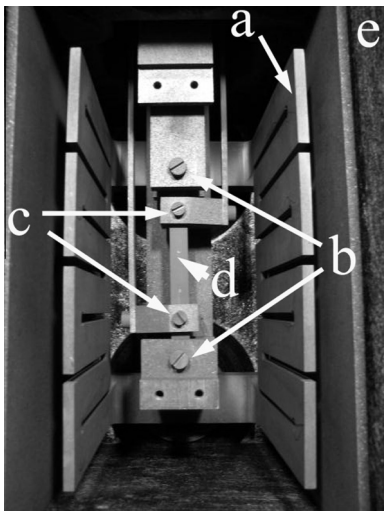


**Fig. 1 – Photo of measurement jigs of high temperature electrical resistance of graphite product in electric furnace, (a) graphite heater, (b) sample support jigs and current probe terminal screw, (c) voltage probe terminal screw, (d) sample specimen, and (e) thermal insulator made from carbon felt composite. This photo is taken the jig removed the front plate.**

A typical temperature dependence curve of electrical resistivity and some specialty parameters estimated from the curve is schematically shown in Fig. 2. In the case of the present graphite products, downward curves of temperature dependence of resistivity are observed, showing the minimum point at certain temperature. Two specialty values, the minimum resistivity ($R_{min}$) and temperature ($T_{min}$), are found from the curve. From Arrhenius plots of the temperature dependence of conductivity (=1/R) in the range from 100 to 300 °C, activation energy for the resistivity decrement was estimated for each product. Beyond the temperature showing the minimum point, on the other hand, a slope of the temperature dependence of resistivity at 1000 °C, $(\Delta R/\Delta T)_{1000\,^\circ C}$, was estimated from the resistivity difference $\Delta R$ ($=R_{1100\,^\circ C} - R_{900\,^\circ C}$), as a parameter for electrical properties under high temperature.

## 3. Results

### 3.1. Relation among XRD structural parameters

The graphitization degree $P_1$ of 12 products is listed in Fig. 3. The plots of XRD structural parameters, $d_{002}$ and Lc, as a function of $P_1$ are shown in Fig. 4. It is reasonably seen to lower $d_{002}$ to 0.3354 nm with the increase in $P_1$ (Fig. 4a). Between

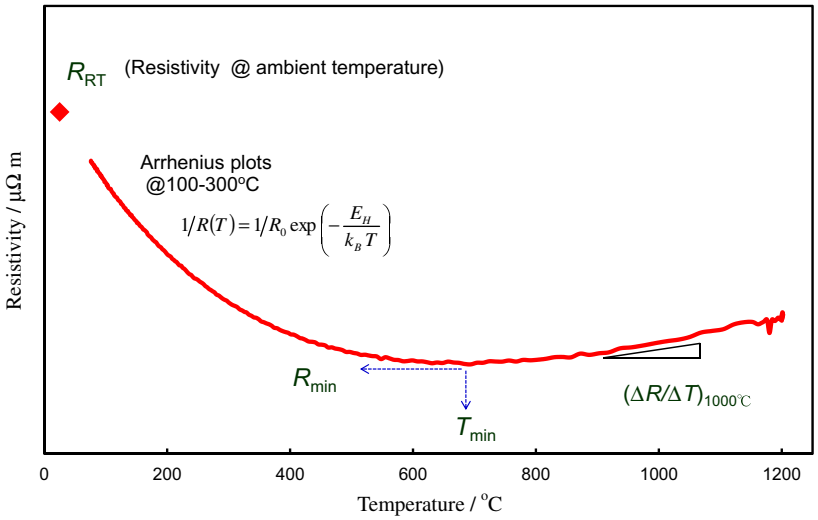


**Fig. 2 – An example of temperature dependence curve of electrical resistance of artificial graphite product and some specialty parameters estimated from the curves.**

$P_1$ and $d_{002}$, it was concluded that an exponential relation was observed on the basis of a number of experimental points for various carbon materials [13]. The value of $P_1$ is the probability for the nearest-neighbor pairs of layers having the graphitic relationship (the ABAB or ABCABC sequences), in other words, the volume fraction of graphitic structure having three-dimensional stacking order, in carbon hexagonal net layers. And $P_1$ has a mutual relation with the structural strain. On the other hands, the $d_{002}$ can be close to the value of natural graphite (=0.3354 nm), even if carbons contain a large amount of structural strain. It was also found that a good relation between $P_1$ and crystallite size along the *c*-axis *Lc* [13]. In case of the present products, however, the samples #6 and #12 are isolated from the relations for the other ten samples, showing relatively small $d_{002}$ and large *Lc*, even in the same value of $P_1$. Fujimoto simulated X-ray scattering intensity of carbon materials with turbostratic stacking and AB stacking structure [15]. From this simulation, it was found that the crystallite size along the *a*-axis *La* had a unique relation with $d_{002}$. In the former report [13], it was observed that development of *La* of real carbon materials had a unique relation with lowering $d_{002}$ to 0.3354 nm, However, the sample #12 is located at the position isolated from the other samples (Fig. 4c).

From these plots between XRD structural parameters, it was reasonably supposed that the samples #6 and #12 are mixtures prepared from relatively well-graphitized filler. Especially, the sample #12 consists of highly-graphitized filler. Moreover, it is affirmed that the samples #3, #4 and #5 have high graphitization degree, by heat-treating at a relatively high temperature in the graphitization process.

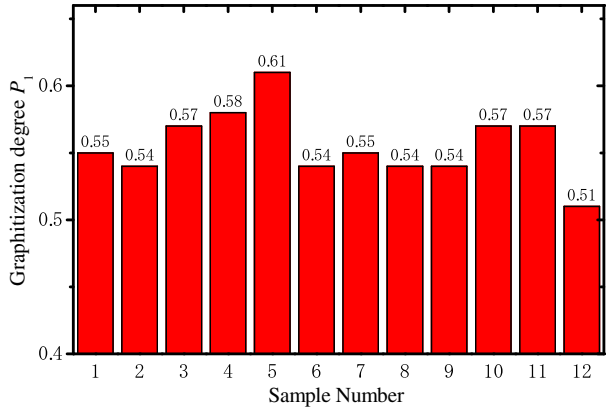


**Fig. 3 – Graphitization degree $P_1$ of 12 artificial graphite products.**

### 3.2. *Relation between temperature dependence of resistivity and XRD structural parameters*

The temperature dependence curves for resistivity of 12 artificial graphite products are shown in Fig. 5. The measured resistivity curves are shown in Fig. 5a and the normalized curves to the ambient value are shown in Fig. 5b. The sample #5, which is the highest $P_1$ among the present samples, shows the smallest ambient resistivity among all of the present products. In the sample #5, moreover, it is characteristic that the resistance at 1200 °C is higher than the ambient value. The sample #12, with the smallest $P_1$ among the present samples, shows the highest resistivity among the present products. In the sample #12, the lowering resistance caused by the elevating temperature is the smallest among the present products.

In Fig. 6, the relation between the resistivity at ambient temperature $R_{RT}$ and XRD structural parameters, $P_1$ and $d_{002}$, are shown. In the plots of $R_{RT}$ against $P_1$, a linear relation, decreasing $R_{RT}$ with the increasing $P_1$, is observed on whole the present samples (Fig. 6a). In the plots against $d_{002}$ (Fig. 6b), except for the samples #6 and #12, the mutual relationship, decreasing $R_{RT}$ with the lowering $d_{002}$ = 0.3354 nm, is observed for the other ten samples. On the other hand, the plots between $R_{RT}$ and $d_{002}$ in the samples #6 and #12 are located at positions isolated from the other ten samples, relatively high ambient resistivity.

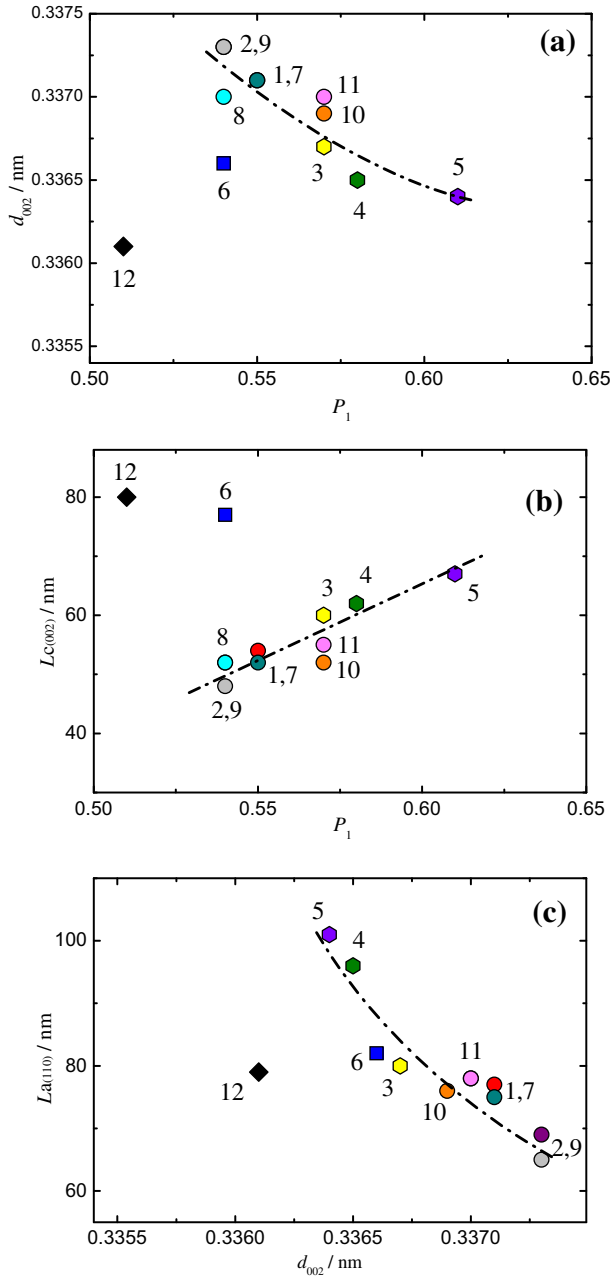


**Fig. 4 – Relations among XRD structural parameters of the graphite products, (a) $P_1$ – $d_{002}$, (b) $P_1$ – Lc and (c) $d_{002}$ – La.**

The plot of the normalized value of the minimum to ambient resistivity, $R_{min}/R_{RT}$, against $d_{002}$ is shown in Fig. 7. The sample #12, showing the smallest interlayer spacing ($d_{002}$ = 0.3361 nm) among the present products, is located the highest value of $R_{min}/R_{RT}$ (=0.83). In the samples #2 and #9, showing the largest interlayer spacing ($d_{002}$ = 0.3373 nm) among the present products, on the other hand, $R_{min}/R_{RT}$ is 0.69. A linear correlation between $R_{min}/R_{RT}$ and $d_{002}$ is observed from the samples #12 to #2 and #9.

The activation energy, $E_H$, is estimated from Arrhenius analysis of the resistivity decrement caused by the elevating temperature range from 100 to 300 °C. The plot of $E_H$ against $d_{002}$ is shown in Fig. 8. The absolute value of the activation energy, $E_H$, is so small, less than 0.02 eV. In the plots between $E_H$ and $d_{002}$, the value of $E_H$ decreases with the lowering $d_{002}$. With the approaching $d_{002}$ = 0.3354 nm, $E_H$ seems to be close to zero.

The tendency that the resistivity decrement caused by the elevating temperature becomes small with the lowering $d_{002}$ coincides with the report that the first decrement becomes obscure with the higher bulk density, reported by Lutcov et al. [1].

For the temperature showing at the minimum resistivity and for the slope of temperature dependence of resistivity at 1000 °C, it was supposed to be suitable correlations with the crystallite size for the carbon hexagonal net contiguity, La. The plot of the temperature showing the minimum resistivity, $T_{mim}$, against the crystallite size along the *a*-axis La of 12 artificial graphite products is shown in Fig. 9. It is observed that the products maintained the larger La indicate the lower $T_{mim}$. The plot of the slope of temperature dependence curves of the resistivity at 1000 °C, $(\Delta R/\Delta T)_{1000\ °C}$, against La is shown in Fig. 10. The slope $(\Delta R/\Delta T)_{1000\ °C}$ seems to be proportional to crystallite size La, although these plots are scattered. In the case of plots against graphitization degree $P_1$, it was observed the almost similar correlations.

## 4. Discussion

The electrical properties of carbon materials exhibit a strong influence on their crystal structure (size, thickness and stacking order of the hexagonal net layers) and texture (aggregation and orientation of the layers), as characterized by X-ray diffraction and electron microscopes. As the consequence of the previous study of the correlation between galvanomagnetic properties (electrical resistivity, magnetoresistance and Hall coefficient measured at 77 K) and graphitization degree $P_1$ using pyrolytic carbons and cokes heat-treated at different temperature [14], the maximum magnetoresistance and Hall coefficient change sign at graphitization degree $P_1$ = 0.5, which reveals a change in electronic conduction from a one-carrier (positive hole) type to a two-carrier (electron and hole) type. In the present study, all of the used artificial graphite products show $P_1 > 0.5$, the graphitic stacking of hexagonal net layers is predominant. In Fig. 6a, a mutual relation was observed between the resistivity at ambient temperature $R_{RT}$ and graphitization degree $P_1$ in the series of graphite products. From this result, it can be supported that the $P_1$ is the average of volume fraction of graphitic structure for all hexagonal carbon net layers, as discussed in the previous papers [13,14]. Therefore, the resistivity at ambient temperature is also the average property of the artificial graphite products. On the other hands, since interlayer spacing $d_{002}$ is analyzed from the diffraction peak position, it has a tendency to be reflected strongly on well-graphitized parts. Indeed, the artificial graphite product #12, composed from highly-graphitized fillers and low-graphitized parts, with the lowest $P_1$ (=0.51) and the smallest $d_{002}$ (=0.3361 nm), shows the highest resistivity at ambient temperature $R_{RT}$ (=17 μΩm) among the present graphite samples.

Some relationships between the temperature dependence of electrical resistivity and XRD structural parameters of the

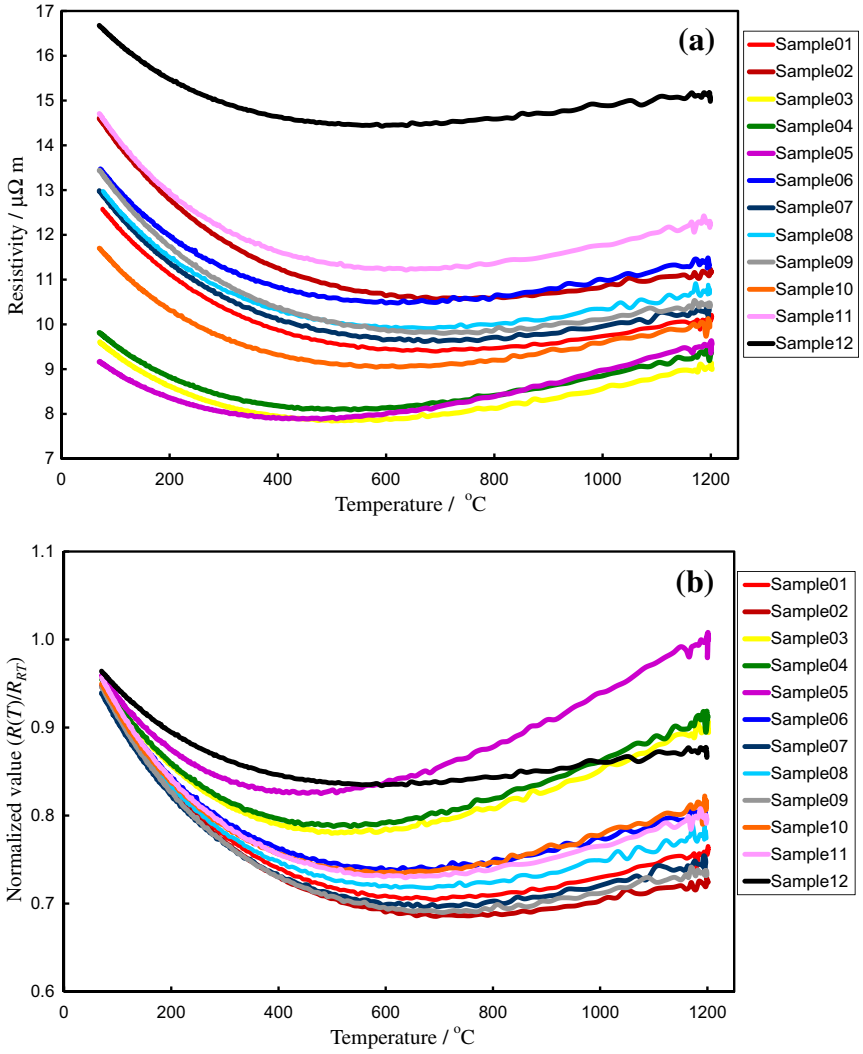


**Fig. 5 – Temperature dependence curves of resistivity of the 12 artificial graphite products, (a) absolute resistivity, and (b) normalized value to ambient temperature.**

series of graphite products was shown in the present study. According to the classical model for conductors, such as metals, electrical conductivity is represented as the mathematical products of carrier density, electrical charge and mobility of carrier. In the artificial graphite samples, the decrement of resistivity with the elevating temperature from ambient to ca. 300 °C is probably due to increment of the carrier density by thermal excitation. However, it is supposed that the mechanism of the increment of the carrier density of the graphite differs from that of hopping conductivity of semiconductors with some band gap, because graphite is semi-metal, of which valence and conduction band are overlapped. Indeed, the absolute value of activation energy $E_H$ for the resistivity decrement was so small (Fig. 8). The normalized value of the minimum to ambient resistivity, $R_{min}/R_{RT,}$ and the activation energy $E_H$ are as functions of interlayer spacing $d_{002}$. With the lowering $d_{002}$, the difference of the minimum from the ambient resistivity became small, in other words, the normalized value ($R_{min}/R_{RT}$) was closed to 1 (Fig. 7). With the lowering $d_{002}$ to 0.3354 nm, the activation energy $E_H$ for the resistivity decrement became small (Fig. 8). It could be suggested that, a contribution of the carrier density increment by thermal excitation to the temperature dependence of resistivity was influenced on interlayer spacing $d_{002}$.

With the elevating temperature beyond the minimum point, the temperature dependence of resistivity turned around. The increment of resistivity may result from a disturbance of carrier motion caused by thermal lattice vibrations of the carbon hexagonal net. This phenomenon occurs at a significantly high temperature. It is reasonably assumed that the disturbance of carrier motion by the thermal vibration can cancel the effect of the carrier density increment caused by thermal excitation, so that the temperature dependence turns around at a certain temperature. This is the reason why the minimum point is observed on the temperature dependence curve of electrical resistivity of the artificial graphite products.

The disturbance of carrier motion caused by the lattice vibration is reasonably assumed to relate to crystallite size along the *a*-axis, La, expanse of carbon hexagonal net. The temperature showing the minimum resistivity, $T_{min}$, and the slope of the temperature dependence at 1000 °C,

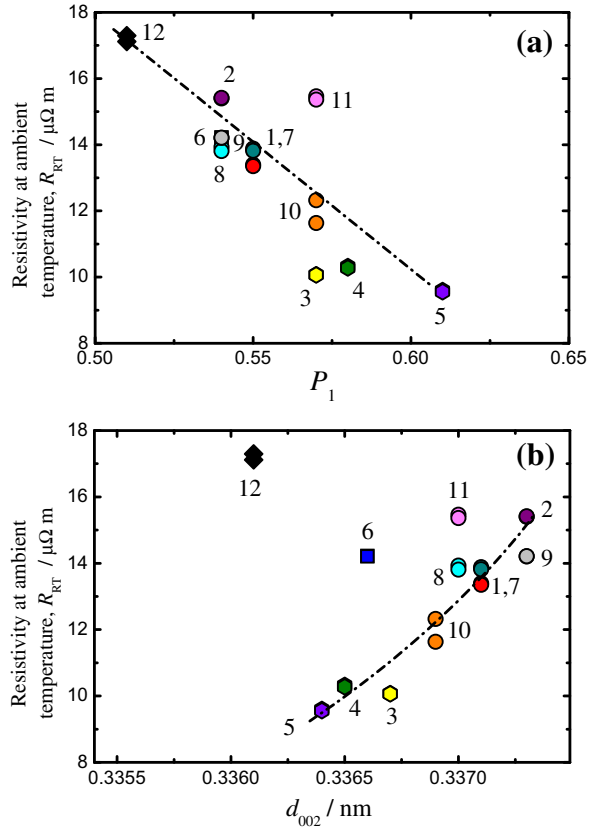


**Fig. 6 – Relations between resistivity at ambient temperature and XRD structural parameters of 12 artificial graphite products, against (a) graphitization degree $P_1$, and (b) interlayer spacing $d_{002}$.**

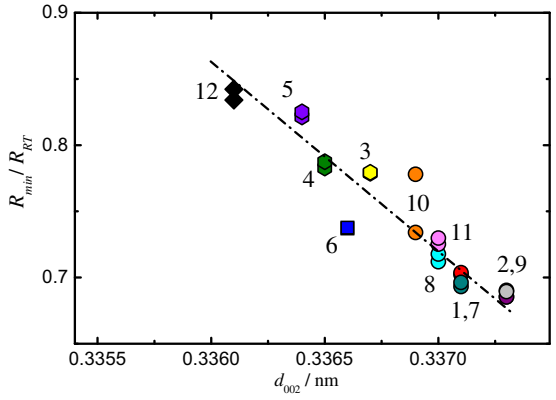


**Fig. 7 – Plot of the normalized value of the minimum to ambient resistivity $R_{min}/R_{RT}$ against interlayer spacing $d_{002}$ of 12 artificial graphite products.**

$(\Delta R/\Delta T)_{1000\ ^\circ C}$, indeed, could be represented as function of *La*. The value of $T_{min}$ shifts to lower side with the increasing *La* (Fig. 9), and the slope $(\Delta R/\Delta T)_{1000\ ^\circ C}$ is proportional to *La* (Fig. 10). In case of a large *La*, therefore, it is reasonably suggested that the carrier disturbance by the lattice vibration is significantly contributed to the temperature dependence of electrical resistivity.

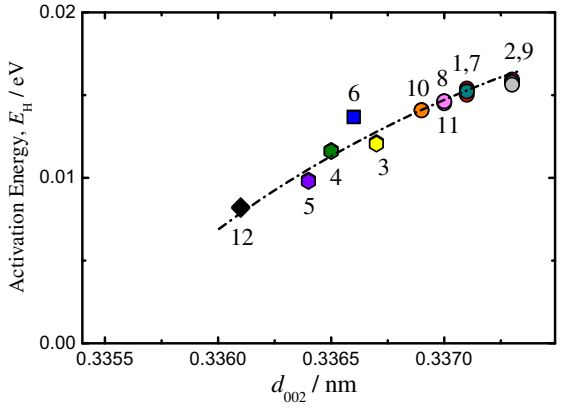


**Fig. 8 – Plot of the activation energy, $E_H$, estimated from Arrhenius analysis of the resistivity decrement with the elevation temperature range from 100 to 300 °C against interlayer spacing $d_{002}$ of 12 artificial graphite products.**

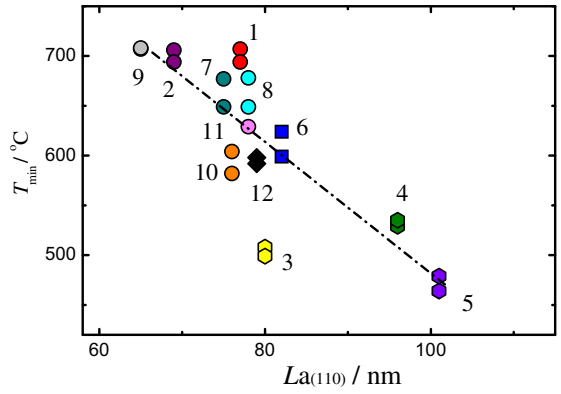


**Fig. 9 – Plot of the temperature showing the minimum resistivity, $T_{mim}$ against crystallite size along the *a*-axis *La* of 12 artificial graphite products.**

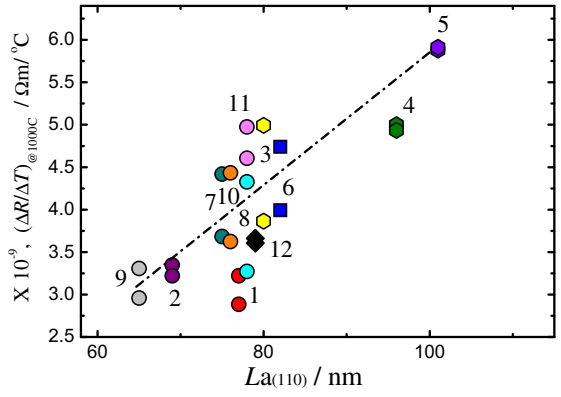


**Fig. 10 – Plot of the slope of temperature dependence curves of the resistivity at 1000 °C against crystallite size along the *a*-axis *La* of 12 artificial graphite products.**

## 5. Conclusion

In the present work, for 12 kinds of artificial graphite products, maintained their graphitization degree $P_1$ from 0.50 to 0.65 and interlayer spacing $d_{002}$ from 0.336 to 0.338 nm, the downward temperature dependence curves of electrical resistivity were observed with the elevation of temperature to 1200 °C. The minimum resistivity points were shown at the temperature region from 450 to 700 °C. Between the resistivity at ambient temperature and graphitization degree $P_1$, a good relation could be observed in all present samples. The graphitization degree $P_1$ is the volume fraction of graphitic structure in artificial graphite products, so that their resistivity, which is related to $P_1$, may be an average property of the products. In the plots of the resistivity at ambient temperature against interlayer spacing $d_{002}$, the samples prepared from well-graphitized filler cokes were shown to shift to low $d_{002}$, as compared with the others, because $d_{002}$ tended to be reflected strongly on well-graphitized parts.

The normalized ratio of the minimum to ambient resistivity, $R_{min}/R_{RT}$, had a correlation with the interlayer spacing $d_{002}$, even in the samples prepared from well-graphitized filler. When the interlayer spacing $d_{002}$ of graphite products was close to 0.3354 nm, the difference between $R_{min}$ and $R_{RT}$ became small. The resistivity decrement with the elevating temperature from ambient to 400 °C might be resulted from the increment of carrier density caused by thermal excitation. Therefore, it was found that a contribution of the carrier increment by the excitation to the temperature dependence of resistivity was influenced on interlayer spacing $d_{002}$.

On the other hand, the resistivity increment with the elevated temperature beyond the minimum point resulted from electric carrier disturbance by thermal lattice vibration. It was assumed that the carrier disturbance by the thermal vibration can cancel the carrier increment by thermal excitation, so that the minimum resistivity occurred at a certain temperature. The temperature showing at the minimum resistivity, $T_{min}$, was lowered with the enlargement of crystallite size along the *a*-axis, *L*a. The slope of temperature dependence of resistivity at 1000 °C, $(\Delta R/\Delta T)_{1000\ ^\circ C}$ was proportional to *L*a in whole graphite products.

## REFERENCES


[1] Lutcov AI, Volga VI, Dymov BK. Thermal conductivity, electric resistivity and specific heat of dense graphite. Carbon 1970;8(6):953–60.

[2] Bapat SG, Nickel H. Thermal conductivity and electrical resistivity of POCO grade AXF-Q1 graphite to 3300 K. Carbon 1973;11(4):323–7.

[3] Bapat SG. Thermal conductivity and electrical resistivity of two types of ATJ-S graphite to 3500 K. Carbon 1973;11(5):511–4.

[4] Iwashita N. Testing of industrial carbon materials under a high temperature. J Mater Test Res Assoc Jpn 2008;53(4):241–6 [Japanese].

[5] Iwashita N. Tensile test of carbon materials at high temperature. J Mater Test Res Assoc Jpn 2011;55(2):76–80 [Japanese].

[6] Iwashita N. Effect of surface roughness on flexural strength of glassy carbons at high temperatures. J Mater Test Res Assoc Jpn 2011;55(4):173–8 [Japanese].

[7] Iwashita N, High temperature tensile test of isotropic graphite blocks, extend abstract for carbon 2011, Shanghai, China, July 25–29; 2011. CD-R, No.154.

[8] Iwashita N, Morikawa, Electrical resistance and thermal diffusivity of isotropic graphite blocks under a high temperature, extend abstract for carbon 2008, Nagano, Japan, July 13–18; 2008. CD-R.

[9] Iwashita N, Park CR, Fujimoto H, Shiraishi M, Inagaki M. Specification for the procedure of X-ray diffraction measurements on carbon materials. Carbon 2004;42(4):701–14.

[10] Warren BE. X-ray diffraction in random layer lattices. Phys Rev 1941;59:693–8.

[11] Houska CR, Warren BE. X-ray study of the graphitization of carbon black. J Appl Phys 1954;25(12):1503–9.

[12] Noda T, Iwatsuki M, Inagaki M. Changes of probabilities $P_1$ $P_{ABA}$, $P_{ABC}$ with heat treatment of carbons. TANSO 1966;47:14–22 [Japanese].

[13] Iwashita N, Inagaki M. Relation between structural parameters by X-ray powder diffraction on various carbon materials. Carbon 1993;31(7):1107–13.

[14] Iwashita N, Inagaki M, Hishiyama Y. Relations between degree of graphitization and galvanomagnetic properties of pyrolytic carbons and cokes. Carbon 1997;35(8):1073–7.

[15] Fujimoto H. Theoretical X-ray scattering intensity of carbons with turbostratic stacking and AB stacking structures. Carbon 2003;41(8):1585–92.